Pflugers Arch - Eur J Physiol (2009) 458:745–759
DOI 10.1007/s00424-009-0667-x

MOLECULAR AND GENOMIC PHYSIOLOGY

Expression patterns of the aquaporin gene family during renal development: influence of genetic variability

Kleber S. Parreira · Huguette Debaix · Yvette Cnops · Lars Geffers · Olivier Devuyst

Received: 28 February 2009 / Accepted: 23 March 2009 / Published online: 16 April 2009

Abstract High-throughput analyses have shown that aquaporins (AQPs) belong to a cluster of genes that are differentially expressed during kidney organogenesis. However, the spatiotemporal expression patterns of the AQP gene family during tubular maturation and the potential influence of genetic variation on these patterns and on water handling remain unknown. We investigated the expression patterns of all AQP isoforms in fetal (E13.5 to E18.5), postnatal (P1 to P28), and adult (9 weeks) kidneys of inbred (C57BL/6J) and outbred (CD-1) mice. Using quantitative polymerase chain reaction (PCR), we evidenced two mRNA patterns during tubular maturation in C57 mice. The AQPs 1-7-11 showed an early (from E14.5) and progressive increase to adult levels, similar to the mRNA pattern observed for proximal tubule markers (Megalin, NaPi-IIa, OAT1) and reflecting the continuous increase in renal cortical structures during development. By contrast, AQPs 2-3-4 showed a later (E15.5) and more abrupt increase, with transient postnatal overexpression. Most AQP genes were expressed earlier and/or stronger in maturing CD-1 kidneys. Furthermore, adult CD-1 kidneys expressed more AQP2 in the collecting ducts, which was reflected by a significant delay in excreting a water load. The expression patterns of proximal vs. distal AQPs and the earlier expression in the CD-1 strain were confirmed by immunoblotting and immunostaining. These data (1) substantiate the clustering of important genes during tubular maturation and (2) demonstrate that genetic variability influences the regulation of the AQP gene family during tubular maturation and water handling by the mature kidney.

Keywords Water handling · Inbred strain · Outbred strain · Mouse kidney

Electronic supplementary material The online version of this article (doi:10.1007/s00424-009-0667-x) contains supplementary material, which is available to authorized users.

K. S. Parreira · H. Debaix · Y. Cnops · O. Devuyst (✉)
Division of Nephrology,
Université catholique de Louvain Medical School,
10 Avenue Hippocrate, 1200 Brussels, Belgium
e-mail: Olivier.Devuyst@uclouvain.be

L. Geffers
Department of Genes and Behavior,
Max Planck Institute for Biophysical Chemistry,
Göttingen, Germany

Introduction

Tubular segmentation and epithelial cell differentiation are essential to ensure the efficient transport of solutes and water by the mammalian kidney. Recent studies, based on global gene expression analyses in rat and mouse, have suggested that major steps of kidney organogenesis are reflected by clusters of differentially regulated genes involved in cellular proliferation and morphogenesis, extracellular matrix synthesis, energy production, and transport processes [32, 36]. The proximal–distal segmentation of the renal tubule involves a group of transport proteins that are upregulated after the onset of glomerular filtration or after birth. These transporters include ATPase subunits, water channels, and organic and inorganic substance transporters [36]. However, high-throughput methods do not allow analyzing the spatiotemporal regulation of gene families during tubular maturation, hence limiting the functional inference of such data.

The issue of segmental differentiation during tubular maturation is particularly relevant when considering the aquaporins (AQPs), a family of integral plasma membrane proteins conserved in bacteria, plants, and mammals, which facilitate water permeation across biological membranes [1]. To date, 13 members of the AQP family (AQP0 to AQP12)

have been identified in mammals, with specific expression patterns and distinct roles in given tissues and cells. Most AQPs are exclusively permeable to water, whereas some isoforms (AQP3, AQP7, AQP9, and AQP10, called "aquaglyceroporins") transport water, glycerol, and urea [15]. It has been recently proposed that AQP11 and AQP12 belong to a subfamily that is localized subcellularly to the endoplasmic reticulum [11]. At least seven AQP isoforms are expressed in distinct nephron segments where they provide pathways for constitutive or vasopressin-activated water transport [15]. Although the ontogeny of selected AQP isoforms has been documented in several species [9, 10, 13, 41], there has been no detailed investigation of the spatiotemporal expression patterns of the AQP gene family during tubular maturation of the mouse kidney.

Most of the genetically modified mouse models have been generated in the C57BL/6J (C57) mouse, the reference inbred strain which was selected for mouse genome sequencing [38]. In principle, the use of an inbred strain such as the C57 allows minimizing the effect of genetic variability on the observed phenotype. By contrast, outbred strains such as the Swiss CD-1 (ICR) are deliberately bred to maintain a high degree of genetic variability which reflects the variation observed in wild mouse (or human) populations [28]. The CD-1 mice, which produce large litters, are widely used in toxicology, oncology, pharmacology, and biomedical research, and their polymorphic loci can be useful in deciphering the mechanisms of gene regulation and complex traits [7]. There is little evidence substantiating the influence of genetic variation on renal function in mouse, and the effect of inbred vs. outbred genetic background on the regulation of a gene family during nephrogenesis is unknown.

In the present study, we performed an extensive analysis of the spatiotemporal expression patterns of the AQP gene family and segmental markers during kidney organogenesis in mouse based on robust quantitative polymerase chain reaction analyses, in situ hybridization, immunoblotting, and immunostaining performed on microdissected embryonic and postnatal kidneys. We also investigated the effect of the genetic background by comparing the expression profiles in the outbred and inbred mouse strains, CD-1 and C57, respectively. Finally, we performed functional studies to demonstrate the influence of the genetic background on water handling and AQP expression in the mature kidney.

Materials and methods

Mouse kidney samples Samples were obtained from inbred C57BL/6J (C57) and outbred Swiss CD-1 (Charles River, L'Arbresle, France) mice in accordance with NIH guidelines for the care and use of laboratory animals and with the approval of the Committee for Animal Rights of the Université catholique de Louvain (Brussels). All mice were housed in identical environments with the same diet (KM-04-K12, Carfil, Goordijk, Belgium). Embryos from five (CD-1, average 12 embryos per litter) and four (C57, average 7 embryos per litter) different litters were collected daily (08:00 to 10:00 A.M.) from embryonic day 13.5 (E13.5) until birth (P1) in order to isolate kidneys by microdissection [13]. Whole kidneys from postnatal P7, P21, and P28 stages and 9-week adult males were also collected. The kidneys were harvested in RNAse-free phosphate-buffered saline (PBS) buffer on ice and immediately frozen in liquid nitrogen. Embryonic kidneys from each litter were pooled into a single sample. Samples were stored at −80°C before protein and RNA extraction. For immunohistochemistry, kidneys were fixed in 4% paraformaldehyde and embedded in paraffin as described [13].

Real-time RT-PCR and data processing Mouse kidney samples were homogenized in Trizol (Invitrogen, Merelbeke, Belgium) in order to extract total RNA. The RNA quality was verified by electrophoresis (Agilent Bioanalyser, Waldbronn, Germany). Total RNA samples were treated with DNase I (Invitrogen) and reverse-transcribed into cDNA using SuperScript II RNase H reverse transcriptase (Invitrogen). Specific primers were designed using Beacon Designer 2.0 (Premier Biosoft International, CA, USA; Electronic supplementary material 1). Real-time PCR analyses were performed in duplicate with 200 nM of both sense and antisense primers in a final volume of 25 µl using 1 U of Platinum Taq DNA Polymerase, 2 mM $MgSO_4$, 400 µM dNTP, and SYBR Green I (Molecular Probe, Leiden, The Netherlands). PCR conditions were incubation at 94°C for 3 min followed by 40 cycles of 30 s at 95°C, 30 s at 61°C, and 1 min at 72°C. The melting temperature of PCR product was checked by recording SYBR green fluorescence increase upon slowly renaturating DNA. For each assay, standard curves were prepared by serial fivefold dilutions of mouse adult kidney cDNA. Efficiency of the amplifications was calculated from the slope of the standard curve $\left[\text{efficiency} = \left(10^{-1/\text{slope}}\right) - 1\right]$ and was close to 100% (Electronic supplementary material 1).

Reference gene analysis was performed using the geNorm [39], Normfinder [3], and BestKeeper [26] programs based on Ct values for β-actin, cyclophilin, GAPDH, HPRT1 genes. Briefly, geNorm allows the most appropriate reference gene to be chosen by using the geometric mean of the expression of the candidate cDNA. All the internal controls are ranked from the lowest to the highest *M* value, the internal control gene stability value, where the lowest represents the most stable gene [39]. BestKeeper also selects the least variable gene using the geometric mean but uses raw data instead of data converted to copy number [26]. All data processing is based on crossing point values that are the

intersections of the threshold line and the amplification curve [27]. Finally, Normfinder measures the variation and ranks the potential reference genes by how much they differ between study samples [3]. For the four internal control genes studied, five independent cDNA samples were amplified for each stage (E13.5 to E18.5, P1, P7, P21, P28, and adult) and introduced in the software packages.

The relative mRNA expression of the housekeeping genes, AQP isoforms and tubular markers was investigated in adult male kidneys ($n=5$), after normalization to GAPDH $\left[\text{Ratio} = 2^{\Delta\text{Ct}(\text{GAPDH}-\text{Target Gene})}\right]$. The relative changes in mRNA levels of these genes during ontogeny were determined by comparison to the adult mRNA level after adjustment to GAPDH [25]:

$$\left[\text{Ratio} = \left(\text{Efficiency}_{\text{target gene}}\right)^{\Delta C_t(\text{Adult}-\text{sample})} \Big/ \left(\text{Efficiency}_{\text{GAPDH}}\right)^{\Delta C_t\ (\text{Adult}-\text{sample})}\right].$$

Antibodies We used well-characterized polyclonal antibodies against AQP1 (Chemicon International, Temecula, CA, USA); AQP2 (Sigma, St. Louis, MO, USA) and Ser256 phosphorylated AQP2 (pAQP2) [2]; AQP3 and AQP4 (a gift from J-M. Verbavatz, CEA/Saclay, Gif-sur-Yvette, France); and a monoclonal anti-β-actin (Sigma).

Immunoblotting analyses Membrane extraction and immunoblotting were performed as previously described [13]. Briefly, kidney samples were homogenized in ice-cold buffer [300 mM sucrose and 25 mM *N*-2-hydroxyethylpiperazine-*N*′-2-ethanesulfonic acid made to pH 7.0 with 1 M tris (hydroxymethyl)aminomethane (Tris)] containing Complete™ (Roche, Vilvoorde, Belgium) protease inhibitors. The homogenate was centrifuged at 1,000×*g* for 15 min at 4°C, and the resulting supernatant was centrifuged at 100,000×*g* for 120 min at 4°C. The pellet was suspended in ice-cold homogenization buffer before determination of protein concentration and storage at −80°C. After resolution by sodium dodecyl sulfate–polyacrylamide gel electrophoresis (SDS-PAGE) and blotting on nitrocellulose, the membranes were incubated overnight at 4°C with primary antibodies, washed, incubated for 1 h at room temperature with appropriate peroxidase-labeled antibodies (Dako, Heverlee, Belgium), washed again, and visualized with enhanced chemiluminescence. Normalization for β-actin was obtained after stripping and reprobing the blots. Specificity of the immunoblot was determined by incubation with non-immune rabbit or mouse IgG (Vector Laboratories, Burlingame, CA, USA) or control ascites fluid (Sigma). All immunoblots were at least performed in duplicate. Densitometry analysis was performed with a StudioStar Scanner (Agfa-Gevaert, Mortsel, Belgium) using the NIH-Image V1-57 software.

Deglycosylation studies were performed on mouse kidney extracts and control glycoproteins (Roche). The samples (15 μg total protein) were incubated for 90 min at 37°C with 12 units of *N*-glycosidase F, as recommended by the manufacturer. endoglycosidase H (Endo H) digestions were also performed on mouse kidney extracts by incubation for 16 h at 37°C with 0.5 units of Endo H. Samples were resuspended in 25 μl of Laemmli sample buffer containing 50 mM dithithreitol, incubated for 12 min at 65°C, and resolved by SDS-PAGE on 12% gels.

Immunostaining After blocking endogenous peroxidase for 30 min with 0.3% H_2O_2, sections were incubated with 10% normal goat serum for 60 min and with primary antibodies diluted in PBS containing 2% bovine serum albumin for 60 min. After washing in 50 mM Tris–HCl, sections were successively incubated with biotinylated secondary anti-IgG antibodies, avidin–biotin peroxidase, and diaminobenzidine or aminoethylcarbazole (Vector Laboratories). Sections were viewed under a Leica DMR coupled to a Leica DC300 digital camera (Leica, Heerbrugg, Switzerland). The specificity of immunostaining was tested by incubation (1) in the absence of primary antiserum and (2) with non-immune rabbit serum or control rabbit or mouse IgG (Vector Laboratories).

In situ hybridization Embryonic (E17.5) and male adult kidneys from C57 mice were collected in ice-cold PBS. Embryonic kidneys were fixed in ethanol/formalin/glacial acetic acid (6:3:1) for 3 h at 4°C, while adult kidneys were fixed in 4% paraformaldehyde for at least 3 days at 4°C. Fixed kidneys were then dehydrated, embedded in paraffin, and sectioned in transversal orientation at 8-μm thickness using a Leica RM 2165 microtome. Sections were deparaffinized in X-tra-Solve (Medite Histotechnik, Burgdorf, Germany), rehydrated, and then treated as described [43]. Primer sequences for the mouse AQP genes templates were obtained from the GenePaint database (www.genepaint.org; Supplementary Material 2). PCR products were sequenced and directly used for in vitro transcription. Riboprobe synthesis and robotic in situ hybridization were carried out using established protocols [43]. The in situ hybridization protocol includes a tyramin–biotin amplification reaction step. The protocol was adjusted for kidney paraffin sections by increasing the proteinase K concentration to 10 mg/ml, using a probe concentration of 300 ng/ml, and increasing the time of color reaction to 3× 12 min. Stained slides were scanned using a Leica DM-RXA2 microscope equipped with the Leica electronic focusing system [5]. Brightfield images were collected with a CCD camera (Hitachi, Tokyo, Japan) and a 20× Leica objective (NA 0.70) for embryonal sections and a 10× Leica objective (NA 0.40) for adult sections. Each image was stored as a

bitmap file and individual images were assembled and saved as TIFF file. The resulting TIFF images with a resolution of 0.8 and 1.6 μm/pixel, respectively, were deposited in GenePaint.

Water handling protocols Plasma and urine samples were obtained at baseline (overnight urine collections in metabolic cages), and the urinary concentrating ability was tested after 24-h water deprivation. The capacity to excrete a water load was tested after i.p. injection of 100 μl/g body weight (BW) of sterile water [2]: Urine was collected under a plastic wrapped container on an hourly basis for the next 8 h. Osmolality was determined using a Fiske Osmometer (Needham Heights, MA, USA).

Statistical analysis Data are presented as means±SEM. Comparisons were made by two-tailed Student's *t* test using Instat3 (Graphpad Software, La Jolla, CA). Values of $P < 0.05$ were considered significant.

Results

Expression profiling of housekeeping genes in developing mouse kidney

Real-time reverse transcriptase PCR (RT-PCR) was performed to establish the relative mRNA expression and stability of four housekeeping genes during C57 and CD-1 mouse kidney development. The expression level and stability values of GAPDH, HPRT1, cyclophilin, and β-actin was determined in six fetal (E13.5 to E18.5), four postnatal (P1, P7, P21, and P28), and one mature kidney sample. Analyses based on the geNorm, BestKeeper, and Normfinder algorithms showed that *Gapdh* was the most stable reporter gene in both strains, as indicated by the lowest *M* value (geNorm), stability value (Normfinder), and coefficient of variation and standard deviation (BestKeeper), respectively (Table 1). *Hprt1* values were close to *Gapdh* in both strains, whereas *Actb* (β-actin) and *CypA* (cyclophilin) genes showed higher values, thus less appropriate for internal controls. Thus, GAPDH is the best housekeeping gene to assess the relative mRNA expression of target genes in mouse kidney maturation.

Influence of the genetic background on AQP expression in the adult kidney

We next investigated the influence of the genetic background on the AQP expression pattern in the adult mouse kidney by comparing mRNA and protein levels in kidneys from 9-week male C57 and CD-1 mice (Fig. 1). Real-time RT-PCR analysis based on two primer sets with similar efficiencies revealed large differences in the expression levels of AQP isoforms in adult kidneys (Fig. 1a and Table 2). The pattern of individual isoform expression was similar in both strains, with a major expression level for AQP1, intermediate levels for AQP2, AQP3, and AQP11, lower levels for AQP4, AQP6, AQP7, and AQP8, and undetectable values for AQP0, AQP5, AQP9, AQP10, and AQP12, corroborating previous studies for mammalian aquaporins [15]. Furthermore, the mRNA abundance of AQP2, AQP3, AQP4, and AQP7 was significantly higher

Table 1 Ranking and relative mRNA expression stability of reference genes in the developing mouse kidney

Rank	geNorm		Normfinder		BestKeeper		
	Gene	*M* value	Gene	Stability value	Gene	CV [% CP]	SD [± CP]
C57							
1	Gapdh	0.593	*Gapdh*	0.349	*Gapdh*	2.38	0.55
2	*Hprt1*	0.614	*Hprt1*	0.360	*Hprt1*	2.81	0.50
3	*Actb*	0.625	*Actb*	0.478	*CypA*	3.24	0.59
4	*CypA*	0.652	*CypA*	0.563	*Actb*	3.34	0.70
CD-1							
1	*Gapdh*	0.576	*Gapdh*	0.289	*Gapdh*	2.46	0.44
2	*Hprt1*	0.580	*Hprt1*	0.297	*Hprt1*	2.65	0.59
3	*CypA*	0.618	*CypA*	0.318	*Actb*	2.90	0.51
4	*Actb*	0.629	*Actb*	0.336	*CypA*	2.92	0.54

Genes are ranked based on their *M* value, stability value, and CV and SD calculated by geNorm, Normfinder, or BestKeeper algorithms, respectively. A lower value indicates more stable reference gene expression. *Gapdh* glyceraldehyde-3-phosphate dehydrogenase, *Hprt1* hypoxantine guanine phosphoribosyl transferase 1, *CypA* cyclophilin A, *Actb* β-actin

Five cDNA samples were amplified for each stage of development.

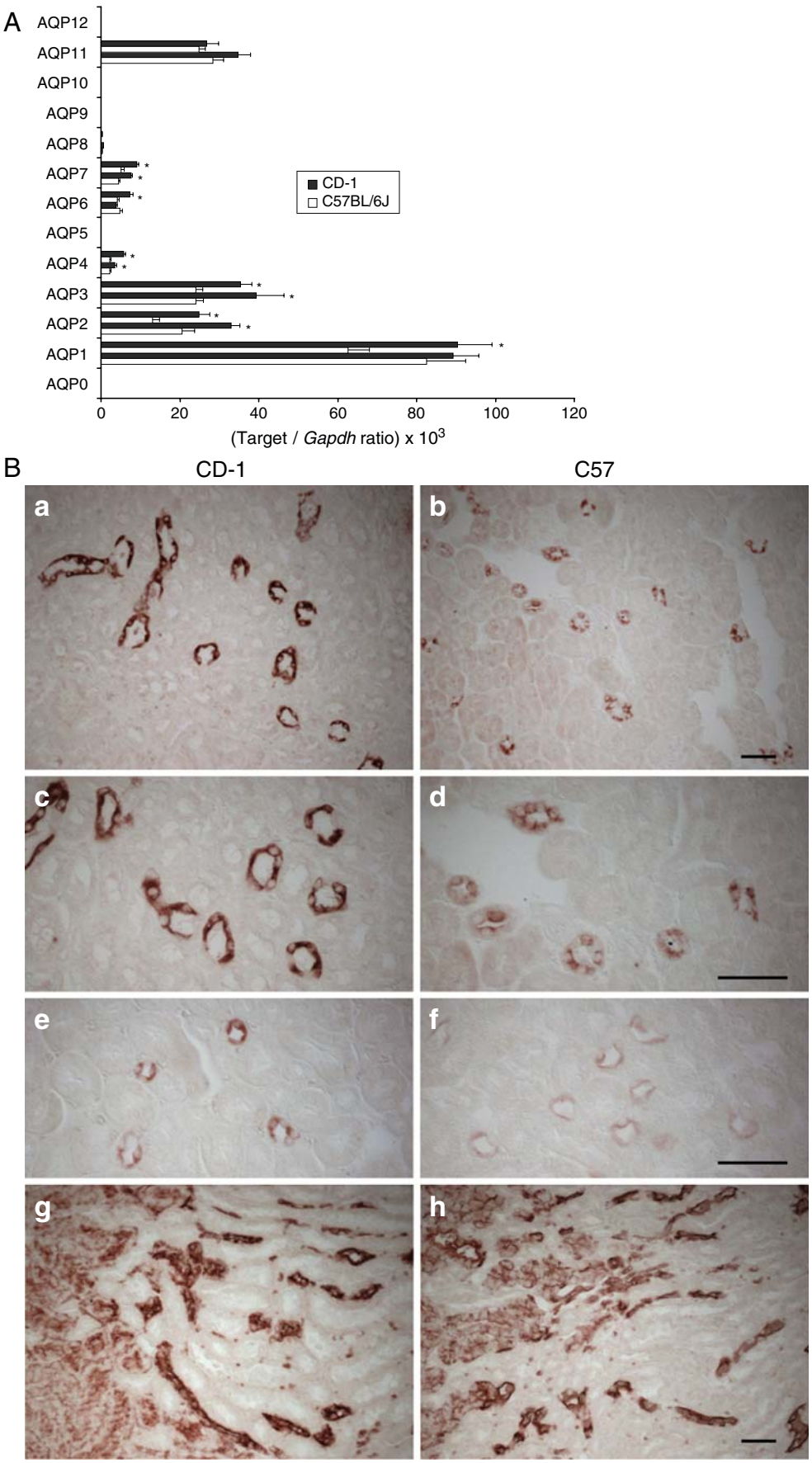

Fig. 1 Influence of genetic background on the expression of AQP isoforms in kidneys of adult C57BL/6J and CD-1 mice. **a** Real-time RT-PCR quantification of AQP isoforms (AQP0 to AQP12) in C57 vs. CD-1 mouse adult kidneys (n=5 individual kidneys for each genotype; *P< 0.05). The values are expressed in [target/reporter gene (*Gapdh*) ratio]×10^3. **b** Immunostaining for AQP2 (**a**–**d**), Ser256 pAQP2 (**e**–**f**), and AQP1 (**g**–**h**) in adult kidneys from CD-1 (*left panels*) and C57 (*right panels*) mice. The representative micrographs show a higher staining intensity for AQP2 and pAQP2 in the collecting ducts (outer medulla) of the CD-1 kidneys, whereas the staining intensity for AQP1 in the proximal tubules and medullary structures (including descending vasa recta and descending thin limbs of long loop nephrons) is similar (**g**–**h**). *Bars* 50 μm

Table 2 Influence of the strain on the relative mRNA abundance of aquaporin isoforms in adult mouse kidney

Gene	PS1		PS2	
	C57	CD-1	C57	CD-1
Aqp0	ND	ND	ND	ND
Aqp1	62.6±5.5	90.3±8.9*	82.5±9.9	89.3±6.5
Aqp2	13.1±1.7	24.9±2.3*	20.5±3.3	33.0±2.2*
Aqp3	24.0±1.8	35.4±2.8*	24.0±1.9	46.4±7.0*
Aqp4	2.3±0.3	5.7±0.5*	2.3±0.3	3.7±0.6*
Aqp5	ND	ND	ND	ND
Aqp6	4.2±0.4	7.3±0.9*	4.8±0.6	3.8±0.3
Aqp7	6.7±0.6	11.0±1.3*	4.5±0.3	7.6±0.3*
Aqp8	0.2±0.0	0.3±0.1	0.3±0.0	0.6±0.1
Aqp9	ND	ND	ND	ND
Aqp10	ND	ND	ND	ND
Aqp11	24.9±1.8	26.8±3.0	28.4±2.6	37.0±3.3
Aqp12	ND	ND	ND	ND

The RNA expression levels were compared after adjustment to glyceraldehyde-3-phosphate dehydrogenase (*Gapdh*; $\times 10^3$) as reporter gene. Significant differences (*$P<0.05$) between C57 and CD-1 are indicated for both sets of primers

PS1 and *PS2* primer set 1 and 2, *ND* non-detected (threshold value fixed <0.05)

in CD-1 vs. C57 kidneys (Fig. 1a). Immunostaining analyses using well-established antibodies (Fig. 1b) confirmed the higher expression of AQP2 and the Ser256 phosphorylated AQP2 in collecting ducts profiles of the mature CD-1 kidney, contrasting with a similar level of AQP1 in the proximal tubules and in medullary structures including descending vasa recta and descending thin limbs (long loop nephrons) [45]. These data reveal that several AQP isoforms are significantly more abundant in mature kidneys of CD-1 mice, including AQP2 in the collecting ducts.

Spatial distribution of aquaporin mRNAs in mouse kidneys

Prior to the analysis of mRNA expression in whole developing kidneys, we documented the segmental distribution of AQP isoforms in E17.5 and mature C57 mouse kidneys by in situ hybridization (Fig. 2). As expected, the AQP1 probe was predominantly distributed in proximal tubules (cortex) and in some medullary structures. Proximal tubules were also stained by the AQP7 and AQP11 probes, although a significant background was produced by the AQP7 probe. The major increase in cortical structures during development was particularly evident for the AQP1 signal. The AQP2 transcript was restricted to medullary and occasional cortical collecting ducts. AQP3 and AQP4 mRNAs were also detected in the collecting ducts where AQP3 was identified in medullary and cortical regions, whereas AQP4 transcript was only observed in the medulla (Fig. 2a). No specific signal was detected for AQP5, AQP9, AQP10, and AQP12 (Fig. 2b), confirming the lack of mRNA detection by RT-PCR in adult kidneys.

Ontogeny of AQP isoforms and tubular maturation in C57 and CD-1 kidneys

The ontogeny patterns of AQP isoforms expressed in the proximal and distal nephron were analyzed during kidney maturation (E13.5 to E18.5) and postnatal development (P1 to P28), in comparison with distinct segmental markers, using real-time RT-PCR analysis (Fig. 3). These studies evidenced two developmental expression patterns, reflecting the distinct segmental origin. The proximal isoforms AQP1, AQP7, and AQP11 showed a continuous and progressive increase from early embryonic stages toward adult levels (Fig. 3a), whereas the distal isoforms AQP2, AQP3, and AQP4 showed a more abrupt increase from E14.5 to E15.5, sustained postnatal overexpression, and downregulation to adult levels (Fig. 3b). Among the distal AQPs, the variations of the AQP2 transcript were particularly sharp, with weak expression at E15.5 reaching the adult level at E17.5, sustained upregulation during postnatal development, and a twofold downregulation to adult levels.

Comparative analysis between C57 and CD-1 strains showed that the expression was either earlier (AQP1, AQP3, AQP4) or significantly higher (all isoforms) during tubular maturation in CD-1 kidneys (see pattern bars in Fig. 3a, b). The strain difference was particularly evident for AQP1 mRNA, first detected at E13.5 and reaching adult level at P7 in CD-1 kidneys, contrasting with later detection (E14.5) and progressive increase towards adult level in the postnatal period in C57 kidneys (Fig. 3a). A similar difference, including earlier expression and faster maturation to adult levels, was observed for the distal AQP3 (Fig. 3b).

In order to gain additional insights into tubular maturation, we also investigated the ontogeny of receptors and transporters with a clearly established segmental distribution (Fig. 4). Quantification of the mRNA expression of the proximal tubule markers, megalin, NaPiIIa, and OAT1, revealed a pattern resembling that of the proximal AQP isoforms, i.e., first detection at E14.5-E15.5, and progressive increase toward adult level during embryogenesis and postnatal maturation (Fig. 4a). These patterns reflected the continuous increase in cortical structures during kidney development. The mRNA expression of the collecting duct markers, AVPR2 and α-ENaC, was similar to the patterns observed for AQP2, AQP3, and AQP4 with early detection, sustained upregulation after birth, and marked dowregulation

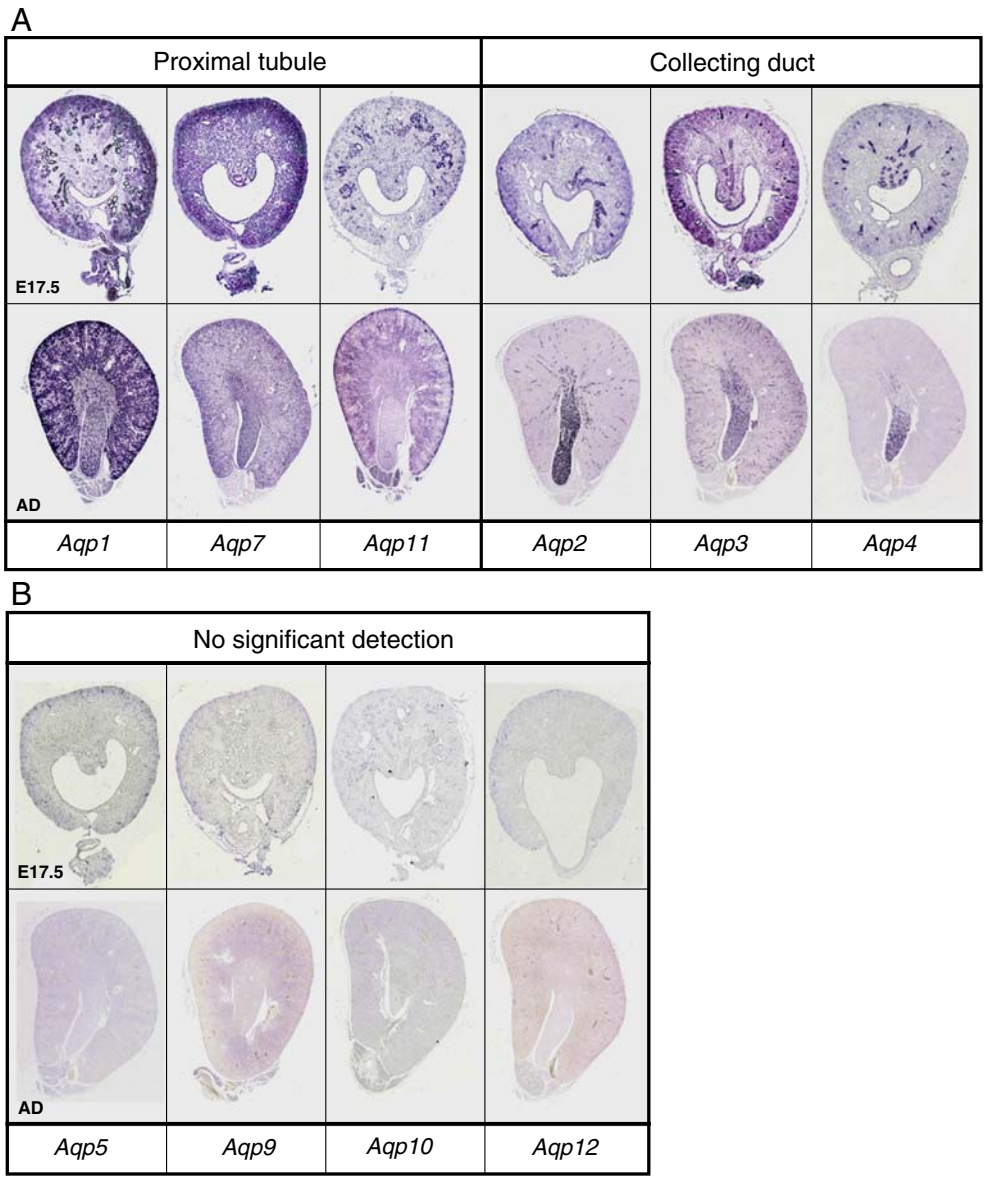

Fig. 2 In situ hybridization for AQP isoforms in developing mouse kidneys. **a** Digoxigenin-labeled antisense probes detected AQP1, AQP7, and AQP11 mRNAs essentially in the cortex (proximal tubules) and faintly in the medulla, whereas AQP2, AQP3, and AQP4 mRNAs are detected in collecting ducts in developing (E17.5) and mature (AD) C57 mouse kidneys. **b** No signal was obtained with the antisense probes for AQP5, AQP9, AQP10, and AQP12

to adult levels at the end of the postnatal period (Fig. 4b). Comparison between strains revealed that megalin expression was higher in CD-1 vs. C57 kidneys for all stages, reaching an approximately fourfold difference in adult kidneys (Fig. 4a). Similarly, OAT1 was approximately twofold more abundant in adult CD-1 kidneys. On the other hand, AVPR2 and α-ENaC were detected earlier or were more abundant in CD-1 kidneys (Fig. 4b).

Taken together, these results suggest that the mRNA expression profiles of AQP genes reflect two specific patterns of ontogeny during proximal tubule and collecting ducts maturation in mouse. Comparison between the C57 and CD-1 strains indicates that there is a significant effect of the genetic background, with earlier and/or higher expression levels for proximal and distal AQP isoforms in the outbred strain.

Time course of aquaporin protein expression and maturation

Immunoblotting analyses were performed to evaluate the expression and maturation of AQP isoforms during kidney development in C57 and CD-1 mice (Fig. 5). The core, non-glycosylated AQP1 (28 kDa) was detected at E16.5 in both strains, with gradual increase during nephrogenesis and detection of the glycosylated isoform (35–50 kDa) after birth (Fig. 5a). By contrast, AQP2 and AQP3 exhibited both glycosylated and non-glycosylated bands roughly at the same developmental stage, with a major increase in the intensity of glycosylated isoforms during the postnatal development (P1–P28). These data support the temporal expression profiles established by real-time RT-PCR, with progressive induction for proximal AQP1 contrasting with

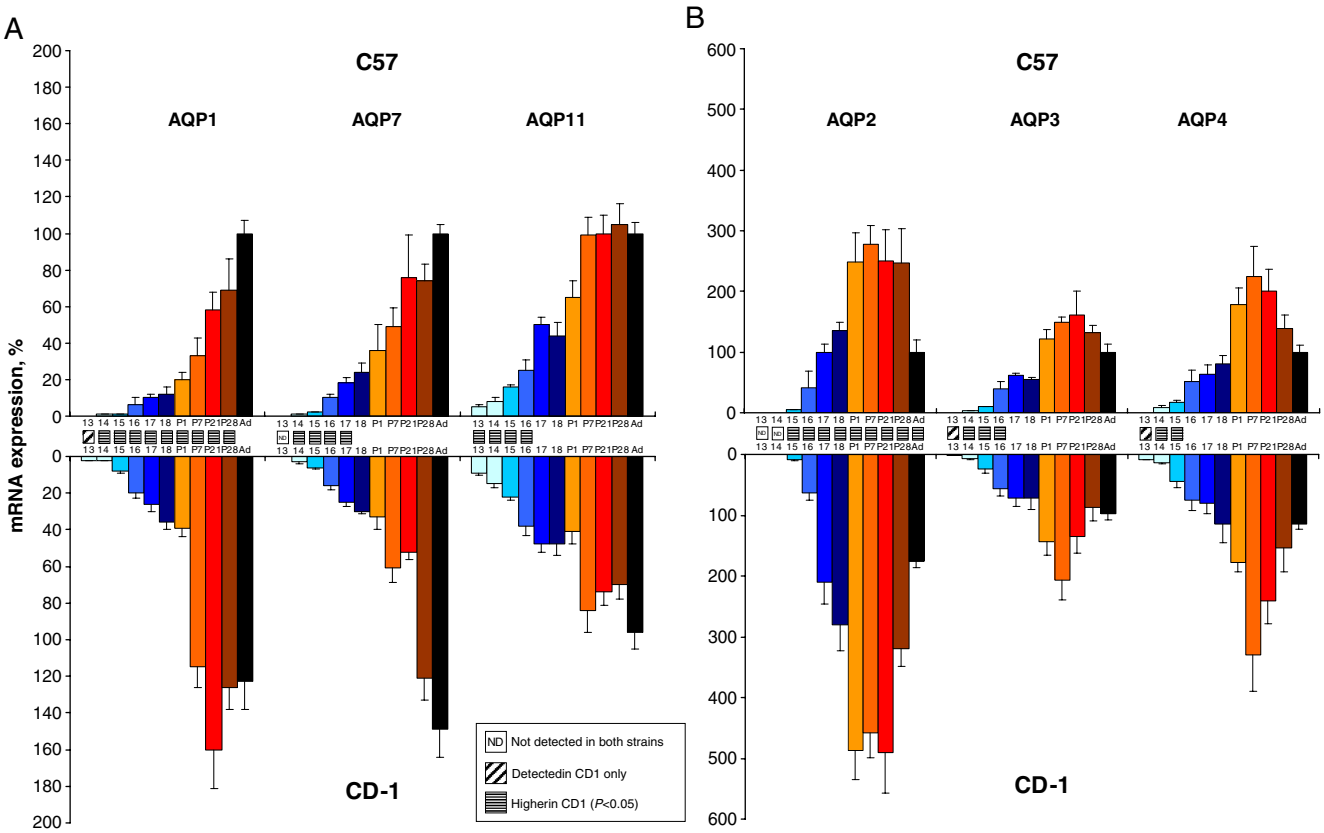

Fig. 3 mRNA expression pattern of AQP isoforms during mouse kidney development and maturation: influence of the strain. Messenger RNA quantification of proximal (**a** AQP1, AQP7, and AQP11) and distal (**b** AQP2, AQP3, AQP4) AQP isoforms in fetal (E13.5 to E18.5, *blue bars*), postnatal (P1 to P28, *orange bars*), and adult (Ad, *black bar*) kidneys of C57 (n=4) and CD-1 (n=5) mouse strains. The mRNA expression levels were first normalized by *Gapdh* at every developmental stage, then adjusted to the adult level set at 100%. Significant differences (P<0.05) between the relative abundance of AQP genes in C57 and CD-1 kidneys are indicated for the appropriate time points

more abrupt increase and postnatal overexpression for the distal AQP2 and AQP3. These profiles are paralleled by two distinct glycosylation patterns during nephrogenesis, with a postnatal and relatively discrete glycosylation of AQP1 contrasting with an earlier and more abundant glycosylation of AQP2 and AQP3.

Comparison between strains revealed that the core AQP1 was detected at E16.5 in C57 and CD-1 kidneys, whereas glycosylated AQP1 bands were more intense in CD-1 at P1 and P7 (Fig. 5a). Similarly, the abundance of glycosylated AQP2 was strikingly higher from E16.5 to E18.5 in CD-1 vs. C57 kidney extracts. Furthermore, both glycosylated and non-glycosylated bands for AQP3 were detected earlier and stronger in the embryonic development of CD-1 vs. C57 kidneys.

In order to examine whether the temporal shift of glycosylation of proximal (AQP1) vs. distal (AQP2 and AQP3) aquaporins was due to segment-specific mechanisms during nephrogenesis, we performed deglycosylation analyses using PNGase F and Endo H. As shown in Fig. 5b, membranes from E16.5, P7, and P28 kidneys consistently displayed a complete deglycosylation of AQP1, AQP2, and AQP3 by PNGase F. For AQP3, a non-glycosylated dimeric band at ~37 kDa was also produced in addition to the expected non-glycosylated band of ~25 kDa [29]. On the other hand, AQP1, AQP2, and AQP3 were clearly insensitive to Endo H for the three developmental stages studied. These results suggest that the aquaporins exclusively undergo *N*-linked glycosylation from early (E16.5) nephrogenesis. Furthermore, as Endo H cleaves high-mannose core sugars of immature proteins that have not exited the endoplasmic reticulum (ER), our data suggest a similar trafficking of AQP1, AQP2, and AQP3 from the ER toward the plasma membrane.

Segmental distribution of aquaporins in C57 and CD-1 kidneys

We next investigated the spatial distribution of AQP1 (Fig. 6) and AQP2 (Fig. 7) protein during nephrogenesis in CD-1 kidneys. AQP1 immunoreactivity was located in the apical membrane of developing proximal tubules and some

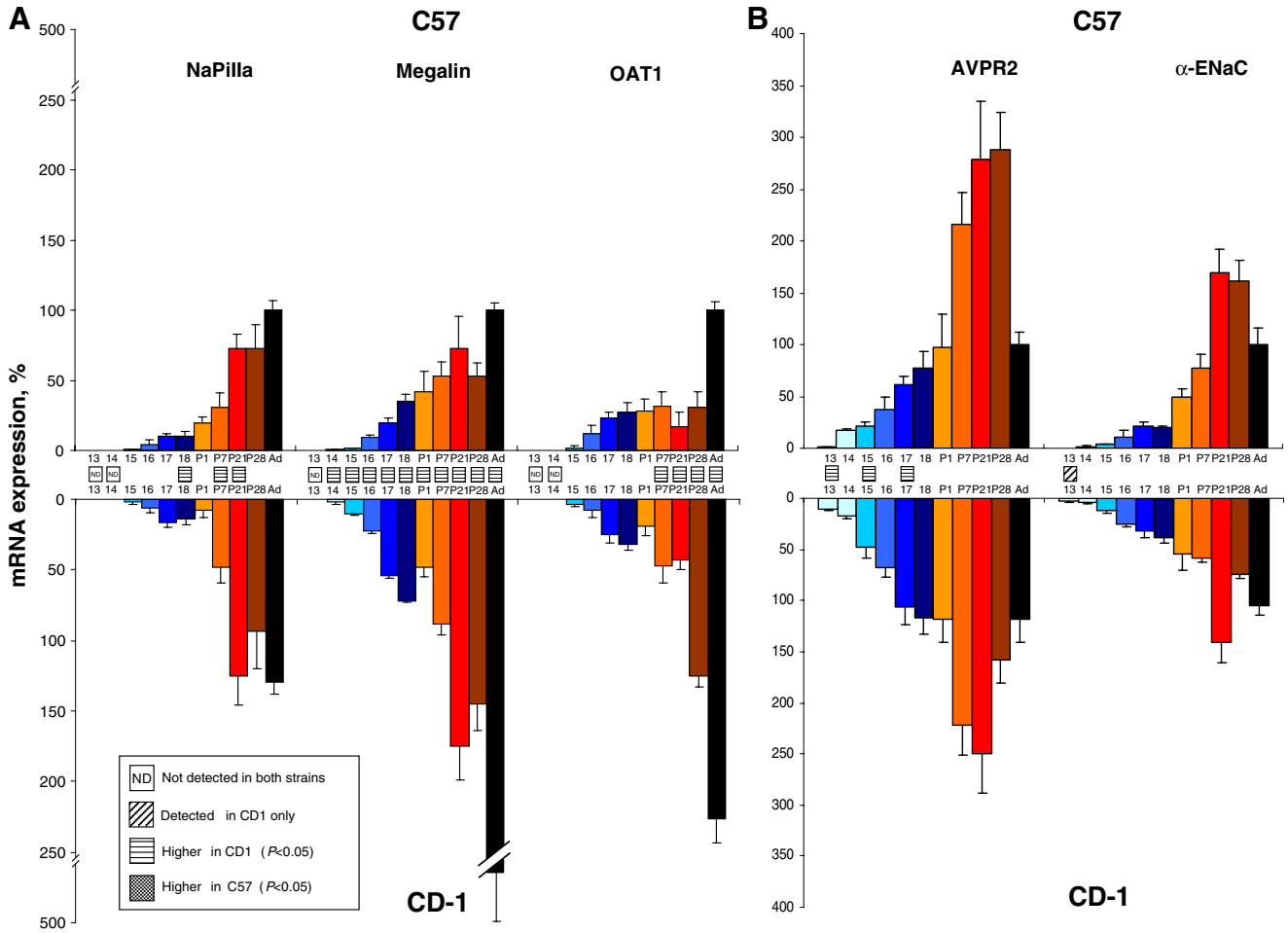

Fig. 4 mRNA expression pattern of tubular markers during mouse kidney development and maturation: influence of the strain. Messenger RNA quantification of proximal (**a** NaPiIIa, megalin, and OAT1) and distal (**b** AVPR2 and α-ENaC) genes in fetal (E13.5 to E18.5, *blue bars*), postnatal (P1 to P28, *orange bars*), and adult (Ad, *black bar*) kidneys of C57 (n=4) and CD-1 (n=5) mouse strains. The mRNA expression levels were first normalized by *Gapdh* at every developmental stage, then adjusted to the adult level set at 100%. Significant differences (P<0.05) between the relative abundance of AQP genes in C57 and CD-1 kidneys are indicated for the appropriate time points

descending thin limbs at E17.5. From E17.5 to P7, and later from P21 to adult stage, a substantial increase in the AQP1-positive tubules was observed in the cortex (Fig. 6). In contrast, positive staining for AQP2 was restricted to the cells lining the collecting ducts in all stages (Fig. 7). At E17.5, AQP2 immunoreactivity was clearly concentrated in the apical membrane region of the collecting ducts cells. A significant increase in AQP2 expression was detected from the sinus to the outer medulla strip from E17.5 until P21, with significant downregulation of the signal in the outer medulla of the adult kidney. Similar distribution patterns were observed in the C57 kidneys (data not shown).

Water handling in adult C57 and CD-1 mice

In order to test whether the significant difference in the expression of AQP2 in the collecting ducts (Fig. 1b) was functionally relevant, we analyzed the water handling in adult CD-1 and C57 mice (Table 3 and Fig. 8). In comparison with age-matched C57 mice, CD-1 mice had a similar urine volume (normalized for body weight), urine osmolality, and urinary creatinine excretion at baseline. Water deprivation induced a similar decrease in urine volume and increase in urine osmolality in both strains (Table 3). However, CD-1 mice showed a significant decrease in their ability to excrete an acute water load at 2 h, with compensatory increase observed after 5–7 h (Fig. 8). The total excreted volume of water after 8 h was similar in both strains (total 8-h urine output, 71±8 % of the water load in C57 vs. 56±5% in CD-1 mice; n=5 pairs). Similar findings were observed in two different series of mice. Thus, the higher expression of AQP2 in the collecting duct of adult CD-1 mice is reflected by a significant shift in the kinetics of water excretion.

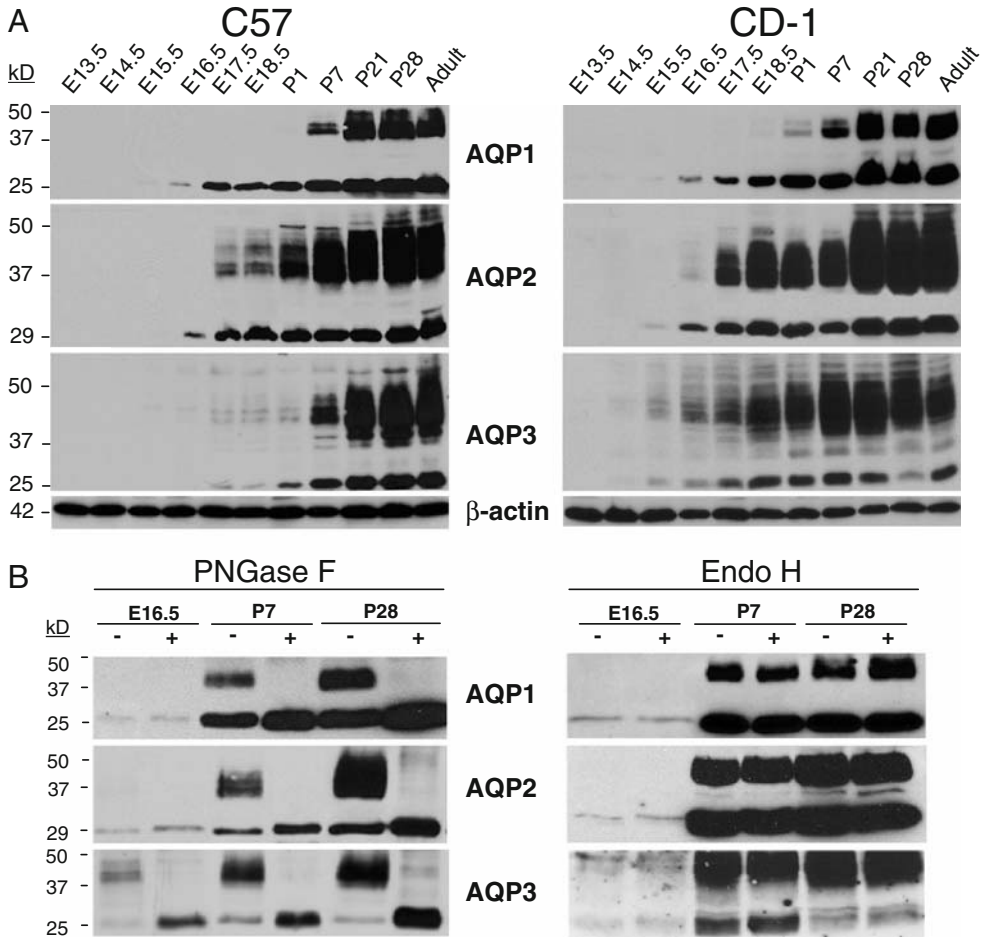

Fig. 5 Expression and maturation of AQP1, AQP2 and AQP3 in the developing mouse kidney: immunoblotting and glycosylation analyses. **a** Representative immunoblotting analyses of AQP expression in membranes fractions of fetal (E13.5 to E18.5), postnatal (P1 to P28), and adult kidneys of C57 vs. CD-1 mouse strains. Equal amounts (20 μg) of protein were loaded in each line, and the blots were probed with anti-AQP1 (1:5,000), anti-AQP2 (1:1,000), anti-AQP3 (1:5,000), and anti-β-actin (1:10,000) antibodies. The AQP bands of about 24 to 28 kDa correspond to the non-glycosylated core, whereas bands of between 37 and 50 kDa correspond to the glyosylated isoforms. **b** Biochemical analysis of AQP1, AQP2, and AQP3 proteins during nephrogenesis. Immunoblot analysis of membrane fractions from CD-1 kidneys at E16.5, P7 and P28 stages. Samples were treated with endoglycosidase F (PNGase F) or endoglycosidase H (Endo H) and equal loads (15 μg) of deglycosylated and non-deglycosylated proteins were analyzed using the same antibodies than in **a**

Discussion

By coupling robust target amplification techniques, in situ hybridization, protein studies, and functional testing, we have investigated the expression and maturation of the AQP gene family in the developing and adult mouse kidney and the influence of genetic variability on these patterns. Our studies reveal specific spatiotemporal patterns of expression of the AQPs during segmental maturation and a significant genetic influence on this regulation. As compared with mature C57 kidneys, CD-1 kidneys show higher expression of AQP2 in the collecting ducts, with a significant difference in water handling.

The accurate analysis of gene expression requires sensitive measurements for specific mRNA sequences, with appropriate PCR conditions and internal controls. For developmental studies, a reporter gene showing maximal stability throughout the development stages despite cellular heterogeneity of the embryo should be selected [46]. Accordingly, we tested the stability of four housekeeping genes based on the geNorm, Normfinder, and BestKeeper algorithms [3, 26, 39]. These analyses showed that *Gapdh*, closely followed by *Hprt1*, is the most stable housekeeping gene (Table 1), justifying its use as reporter during mouse nephrogenesis. By contrast, *Actb*, the classical housekeeping gene coding for β-actin, showed the least stability, in agreement with recent studies in mouse oocytes and preimplantation stage embryos [19].

Analysis of the relative abundance of AQP transcripts in the adult kidney indicated that eight out of 13 AQP isoforms were detected (Fig. 1a and Table 2). The lack of detection of AQP0, AQP5, AQP9, and AQP12 corroborates

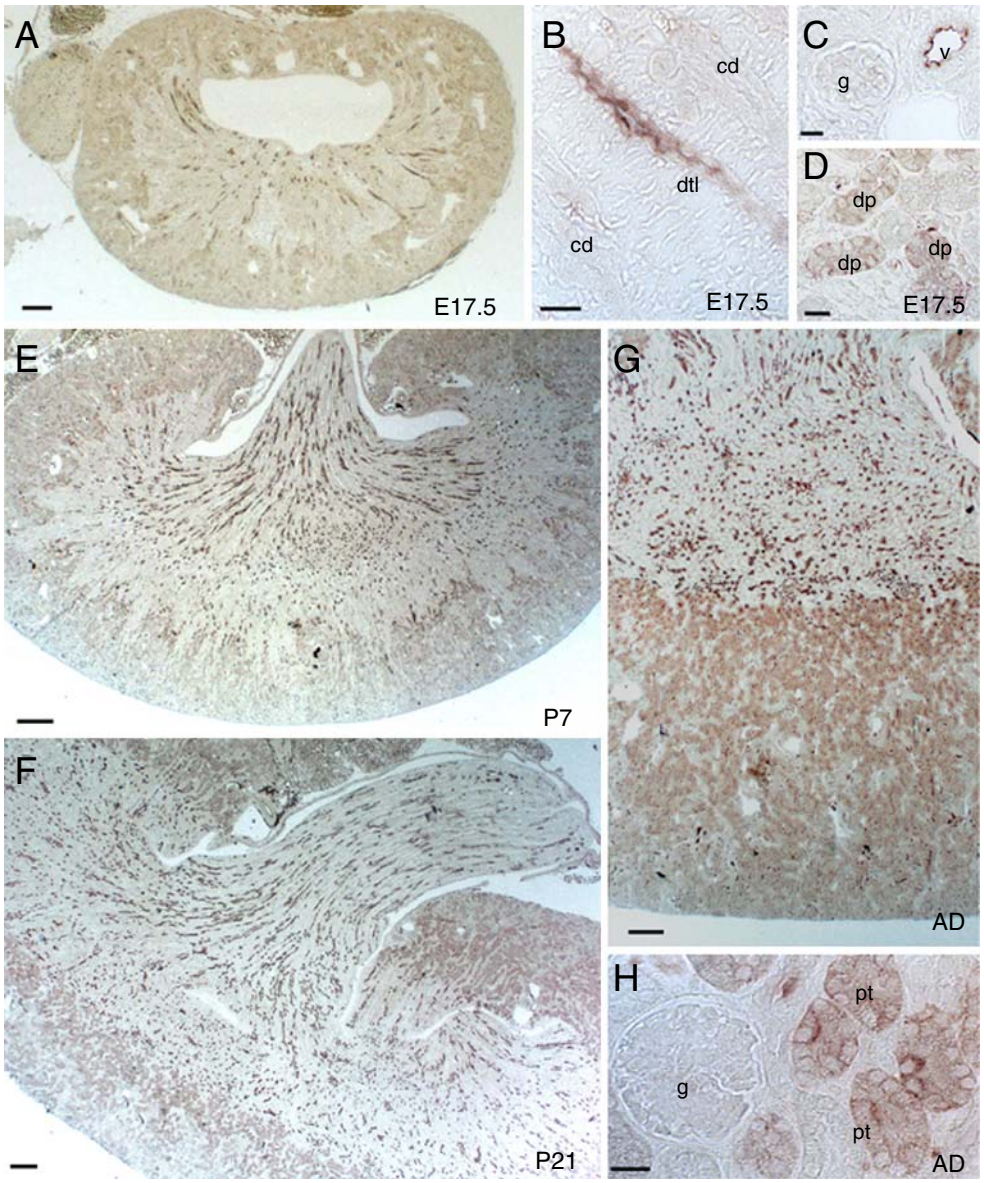

Fig. 6 Segmental distribution of AQP1 during CD-1 mouse nephrogenesis. **a**–**d** Immunostaining for AQP1 (1:200) at E17.5. AQP1 immunoreactivity is detected in some medullary descending thin limb (*dtl*) and developing proximal tubules (*dp*) at E17.5. Glomeruli (*g*) and collecting duct (*cd*) are unstained. Luminal surface of blood vessels (*v*) are strongly stained. **e**–**h**. Postnatal increase in the density of AQP1-positive tubule profiles in the cortex and medulla at P7 (**e**), P21 (**f**), and in adult (**g**–**h**). *Scale bars* 200 μm

the patterns described in previous studies [15], whereas AQP10 is known as a pseudogene that is not expressed in mouse kidney. AQP1 mRNA is by far the most abundant isoform in the adult kidney, in keeping with data suggesting that it constitutes almost 1% of the total membrane proteins of the proximal tubule [23]. By contrast, AQP7, which is expressed in the apical membrane of the proximal straight tubules (S3 segment) [12], is faintly detected. This quantitative difference is in line with the functional role of these isoforms, as knockout experiments indicated that transcellular water transport in the cortex is almost restrictively provided by AQP1 [31], whereas the contribution of AQP7 is minimal [34]. We also observed a strong expression of AQP11 in mouse kidney. AQP11 is localized intracellularly in the ER of proximal tubule cells, and its disruption leads to early postnatal death caused by multiple cysts derived from proximal tubules [21].

Our studies reveal that the mRNA expression of distal AQP isoforms, including AQP2, is significantly higher in mature CD-1 compared to C57 kidneys (Fig. 1a). The PCR efficiencies showed only minimal variations between strains that cannot account for the differences observed. Immunostaining confirmed the higher expression of AQP2 and its Ser256 phosphorylated isoform in the principal cells of the outer medullary collecting ducts (Fig. 1b). Furthermore, the adult CD-1 mice showed a significant delay in handling an acute water load (Fig. 8). Taken together, these data show that the genetic variability of the outbred CD-1 strain influences the regulation of specific AQP isoforms and the capacity of water handling in the adult kidney. The influence of strain on gene expression has been previously demonstrated in various organs from mouse, rat, and other species [30, 40]. However, the evidence for such a variation in the kidney is limited. A recent microarray study de-

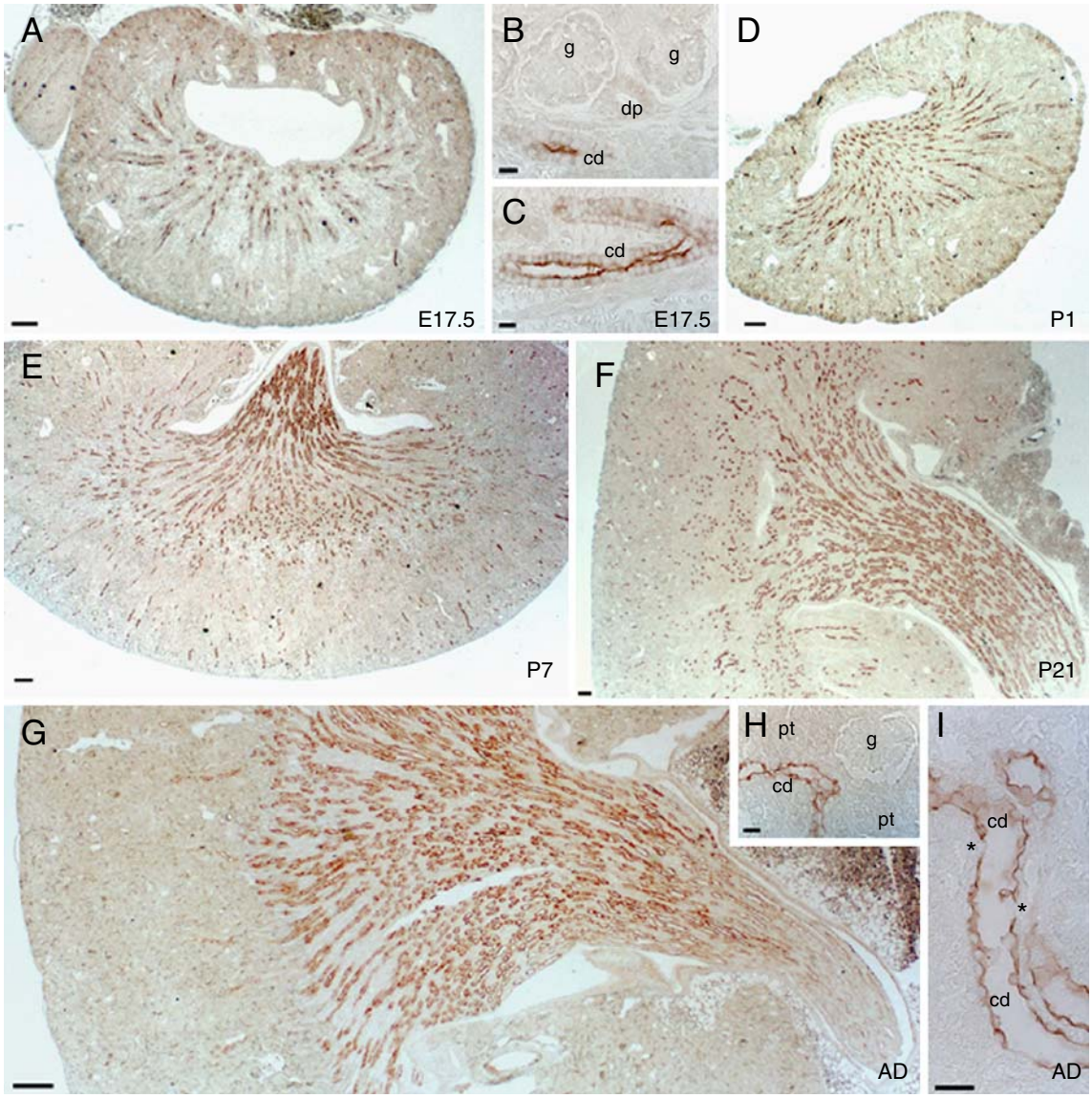

Fig. 7 Segmental distribution of AQP2 during CD-1 mouse nephrogenesis. **a**–**c** Immunostaining for AQP2 (1:200) at E17.5. AQP2 immunoreactivity is detected in collecting ducts (*cd*). Glomeruli (*g*) and developing proximal tubules (*dp*) are negative. **d**–**f** Postnatal increase in AQP2 staining in the medulla, located in collecting ducts profiles at P1 (**d**), P7 (**e**), and P21 (**f**). **g**–**i** Adult kidneys with AQP2 staining in the collecting ducts (*cd*) (**g**, **h**) with negative proximal tubules (*pt*). Note the negative intercalated cells (*asterisk*) in the collecting ducts of mature kidney (**i**). *Scale bars* 200 μm

scribed several genes, including SLC transporters and hormonal regulators, that were differentially regulated in outbred (SD) vs. inbred (F344) rat kidneys [33]. Using RT-PCR, Kunert-Keil et al. [16] showed specific variations in TRP channel isoforms in the kidneys of three inbred mouse strains. Of interest, the inbred C57 line is characterized by its sodium sensitivity, whereas the outbred CD-1 is sodium-resistant, reflecting different responses of the tubular renin–angiotensin system to sodium intake [17]. The CD-1 males are also known to be resistant to estrogen suppression of testicular function when compared to C57 mice, pointing to major genetic differences in endocrine regulation [35].

Analysis of the ontogeny patterns of the AQP gene family revealed a continuous and progressive increase toward adult expression levels for the AQP1, AQP7, and AQP11 genes predominantly expressed in the proximal tubule (Fig. 3a). The most obvious explanation for this pattern is the ~25-fold increase in renal cortical volume from E13.5 to birth, as demonstrated by morphometry [6]. This hypothesis is supported by the similar expression profiles obtained for proximal tubule markers, including megalin, NaPiIIa, and OAT-1 (Fig. 4a), and the massive increase in AQP1 immunoreactivity in cortical tubular structures from E17.5 (Fig. 6). By contrast, quantitative

Table 3 Urinary parameters in adult CD-1 and C57 mice: effect of water deprivation

	C57	CD-1	*P* value
Baseline			
Body weight (g)	27.4±0.8	41.3±1.6	<0.0001
Kidney weight (mg/g body weight)	7.2±0.2	8.3±0.1	0.003
Water intake (ml/12 h)	2.97±0.75	6.57±1.4	<0.05
Urine volume (µl/12 h)	1402±285	3585±995	0.03
Urine volume (µl/12 h/g BW)	50.9±9.6	89.2±27	NS
Urine osmolality (mOsmol/kgH_2O)	2470±332	2017±340	NS
Urine creatinine (µg/12 h/g BW)	25.8±4.2	27.7±3.6	NS
Water deprivation			
Urine volume (µl/24 h/g BW)	20.7±2.9	28.8±3.2	NS
Urine osmolality (mOsmol/kgH_2O)	3355±201	3541±52	NS

Data are expressed as means± SEM, obtained on six pairs of age-matched adult males. Baseline data were obtained overnight in metabolic cages; water deprivation was performed over 24 h

NS not significant, *BW* body weight

mRNA analysis revealed a distinct pattern for the AQP2, AQP3, and AQP4 genes that are predominantly expressed in the collecting ducts. Compared with proximal AQP isoforms, these genes were detected later, with a sharp increase around birth and a significant downregulation during postnatal development (Fig. 3b). Similar findings had been observed in the developing rat kidney [4]. Changes in the relative mass of the medulla during the course of nephrogenesis may explain these findings [6]. Modifications in the vasopressin–AVPR2 pathway might also play a role. Vasopressin regulates AQP2 and AQP3 expression in the adult kidney [22] and injection of dDAVP upregulates AQP2 mRNA levels in maturing rat kidney [42]. Indeed, we show that the expression patterns of AQP2 and AVPR2 are similar, with early postnatal induction followed by downregulation in adult (Fig. 4b). It should be pointed, however, that AVPR2-null mice show an apparently normal expression of AQP2 despite a reduced urine concentrating ability [44].

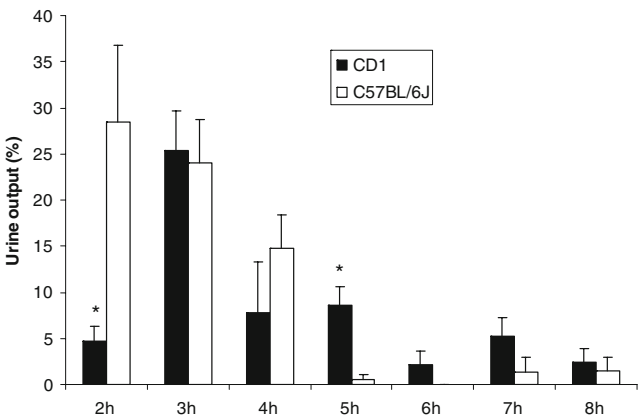

Fig. 8 Response to water loading in C57 and CD-1 adult mice. Six pairs of mice were injected i.p. with 100 µl/g BW of sterile water. In comparison with C57 mice, the CD-1 mice showed a significantly delayed excretion of water up 2 h after the load, with a compensatory increase at later stages (*P<0.05)

Differences in the glycosylation pattern of AQP isoforms (Fig. 5) raise the issue of glycosylation mechanisms during kidney development. The fact that inherited disorders affecting transport proteins (such as NKCC2 and ROMK in Bartter syndrome) are associated with renal dysfunction and polyhydramnios indicates that these transporters are functional—and thus presumably glycosylated and appropriately targeted to the plasma membrane—during late nephrogenesis. Our data suggest that N-linked glycosylation events may occur later in the proximal tubule (AQP1) than in the collecting duct (AQP2, AQP3) during nephrogenesis. In mammalian cells, N-linked glycosylation of proteins is catalyzed by the oligosaccharyltransferase (OST) complex which is constituted by seven subunits including ribophorins I and II, Ost48, Ost3, Stt3A/Stt3B, and Dad1 [14]. Tissue- and cell-type-specific differences in the expression of OST subunits may ensure glycan heterogeneity. Thus, a differential expression of OST subunits in tubular cells might explain different glycosylation patterns during nephrogenesis. This hypothesis is supported by in silico analyses of the GUDMAP microarray expression database [20]. Indeed, the Dad1 subunit, which is essential to the function and the structural integrity of the OST complex [14], is significantly more abundant in medullary collecting ducts than in proximal tubules at E15.5 (data not shown).

Our data support a role of genetic variability in regulating gene expression during kidney development. Several AQP isoforms, both in proximal (AQP1) and distal (AQP3 and AQP4) segments, were detected one developmental stage later in C57 as compared to CD-1 kidneys, both at the mRNA and protein levels (Figs. 3 and 4). A similar feature has been observed in embryonic mouse colon, with C57 samples lagging behind CD-1 samples with respect to developmental maturation [24]. Whether the differences in the AQP gene expression pattern reflect differences in the timing of tubular maturation remains an open question. At any rate, our data support the view that AQP isoforms are reliable markers of tubular segmentation [9, 13, 36], and a delayed detection in

C57 kidney could suggest a later start of tubular maturation as compared with CD-1. It is generally acknowledged that glomerular filtration starts at E14.5 in C57 mice, followed by maturation of the developing proximal tubules [18]. The detection of AQP1 mRNA at E13.5 in CD-1 kidneys implies expression in epithelial condensations and/or developing proximal tubules before the onset of glomerular filtration, unless the metanephric glomeruli become functional at E13.5 in these mice.

Finally, our results should be interpreted considering the high level of genetic variation found in the outbred CD-1 strain, arguably similar to that found in natural mouse and human populations [28]. Differences in genetic background affect the expression levels of a subset of genes in different strains [37], and these differences are apparently tissue-specific [8]. Of interest is that a study of the transcriptome of hindlimb muscle in five inbred mouse strains revealed that the most significant differences, confirmed by quantitative RT-PCR, were determined by low gene expression levels of C57 compared to other strains [37]. Deciphering the genetic counterpart of the differences in AQP gene expression patterns in the kidney is outside the scope of this study. However, the strain variation in AQP gene expression and water handling by the kidney emphasizes the need for careful selection and characterization of mouse models used for renal studies.

Acknowledgments The authors are grateful to Drs. L. Bankir, D. Bichet and all members of the Genepaint In Situ Hybridization Group for their help. These studies were supported by the Belgian agencies FNRS and FRSM (3.4.592.06F), the "Fondation Alphonse & Jean Forton," a Concerted Research Action (05/10-328), an Inter-university Attraction Pole (IUAP P6/05), and the EuReGene (FP6, GA#5085) and EUNEFRON (FP7, GA#201590) programs of the European Community.

References

1. Agre P (2004) Aquaporin water channels (Nobel Lecture). Angew Chem Int Ed Engl 43:4278–4290
2. Ahrabi AK, Terryn S, Valenti G et al (2007) PKD1 haploinsufficiency causes a syndrome of inappropriate antidiuresis in mouse. J Am Soc Nephrol 18:1740–1753
3. Andersen CL, Jensen JL, Orntoft TF (2004) Normalization of real-time quantitative reverse transcription-PCR data: a model-based variance estimation approach to identify genes suited for normalization, applied to bladder and colon cancer data sets. Cancer Res 64:5245–5250
4. Baum MA, Ruddy MK, Hosselet CA, Harris HW (1998) The perinatal expression of aquaporin-2 and aquaporin-3 in developing kidney. Pediatr Res 43:783–790
5. Carson JP, Thaller C, Eichele G (2002) A transcriptome atlas of the mouse brain at cellular resolution. Curr Opin Neurobiol 2002 (12):562–565
6. Cebrian C, Borodo K, Charles N, Herzlinger DA (2004) Morphometric index of the developing murine kidney. Dev Dyn 231:601–608
7. Chia R, Achilli F, Festing MFW, Fisher EM (2005) The origins and uses of mouse outbred stocks. Nat Genet 37:1181–1186
8. Cotsapas CJ, Williams RB, Pulvers JN et al (2006) Genetic dissection of gene regulation in multiple mouse tissues. Mamm Genome 17:490–495
9. Devuyst O, Burrow CR, Smith BL et al (1996) Expression of aquaporins-1 and -2 during nephrogenesis and in autosomal dominant polycystic kidney disease. Am J Physiol Renal Fluid Electrolyte Physiol 271:F169–F183
10. Gattone VH 2nd, Maser RL, Tian C, Rosenberg JM, Branden MG (1999) Developmental expression of urine concentration-associated genes and their altered expression in murine infantile-type polycystic kidney disease. Dev Genet 24:309–318
11. Ishibashi K (2006) Aquaporin subfamily with unusual NPA boxes. Biochim Biophys Acta 1758:989–993
12. Ishibashi K, Kuwahara M, Gu Y et al (1997) Cloning and functional expression of a new water channel abundantly expressed in the testis permeable to water, glycerol, and urea. J Biol Chem 272:20782–20786
13. Jouret F, Igarashi T, Gofflot F et al (2004) Comparative ontogeny, processing, and segmental distribution of the renal chloride channel, ClC-5. Kidney Int 65:198–208
14. Kelleher DJ, Gilmore R (2006) An evolving view of the eukaryotic oligosaccharyl-transferase. Glycobiology 16:47R–62R
15. King LS, Kozono D, Agre P (2004) From structure to disease: the evolving tale of aquaporin biology. Nat Rev Mol Cell Biol 5:687–698
16. Kunert-Keil C, Bisping F, Krüger J, Brinkmeier H (2006) Tissue-specific expression of TRP channel genes in the mouse and its variation in three different mouse strains. BMC Genomics 7:159
17. Lantelme P, Rohrwasser A, Gociman B et al (2002) Effects of dietary sodium and genetic background on angiotensinogen and renin in mouse. Hypertension 39:1007–1014
18. Loughna S, Landels E, Woolf AS (1996) Growth factor control of developing kidney endothelial cells. Exp Nephrol 4:112–118
19. Mamo S, Gal AB, Bodo S, Dinnyes A (2007) Quantitative evaluation and selection of reference genes in mouse oocytes and embryos cultured in vivo and in vitro. BMC Dev Biol 7:14
20. McMahon AP, Aronow BJ, Davidson DR et al (2008) GUDMAP: the genitourinary developmental molecular anatomy project. J Am Soc Nephrol 19:667–671
21. Morishita Y, Matsuzaki T, Hara-chikuma M et al (2005) Disruption of aquaporin-11 produces polycystic kidneys following vacuolization o the proximal tubule. Mol Cell Biol 25:7770–7779
22. Murillo-Carretero MI, Ilundain AA, Echevarria M (1999) Regulation of aquaporin mRNA expression in rat kidney by water intake. J Am Soc Nephrol 10:696–703
23. Nielsen S, Pallone T, Smith BL et al (1995) Aquaporin-1 water channels in short and long loop descending thin limbs and in descending vasa recta in rat kidney. Am J Physiol 268:F1023–F1037
24. Park YK, Franklin JL, Settle SH et al (2005) Gene expression profile analysis of mouse colon embryonic development. Genesis 41:1–12
25. Pfaffl MW (2001) A new mathematical model for relative quantification in real-time RT-PCR. Nucleic Acids Res 29:e45
26. Pfaffl MW, Tichopad A, Prgomet C, Neuvians TP (2004) Determination of stable housekeeping genes, differentially regulated target genes and sample integrity: BestKeeper–Excel-based tool using pair-wise correlations. Biotechnol Lett 26:509–515
27. Rasmussen R (2001) Quantification on the LightCycler instrument. In: Meuer S, Wittwer C, Nakagawara K (eds) Rapid cycle real-time PCR: methods and applications. Springer, Heidelberg, pp 21–34
28. Rice MC, O'Brien SJ (1980) Genetic variance of laboratory outbred Swiss mice. Nature 283:157–161
29. Roudier N, Verbavatz JM, Maurel C, Ripoche P, Tacnet F (1998) Evidence for the presence of aquaporin-3 in human red blood cells. J Biol Chem 273:8407–8412

30. Sandberg R, Yasuda R, Pankratz DG et al (2000) Regional and strain-specific gene expression mapping in the adult mouse brain. Proc Natl Acad Sci U S A 97:11038–11043
31. Schnermann J, Chou CL, Ma T et al (1998) Defective proximal tubular fluid reabsorption in transgenic aquaporin-1 null mice. Proc Natl Acad Sci U S A 95:9660–9664
32. Schwab K, Patterson LT, Aronow BJ et al (2003) A catalogue of gene expression in the developing kidney. Kidney Int 64:1588–1604
33. Seidel SD, Hung SC, Lynn Kan H, Bhaskar Gollapudi B (2006) Background gene expression in rat kidney: influence of strain, gender, and diet. Toxicol Sci 94:226–233
34. Sohara E, Rai T, Miyazaki J et al (2005) Defective water and glycerol transport in the proximal tubules of AQP7 knockout mice. Am J Physiol Renal Physiol 289:F1195–F1200
35. Spearow JL, Doemeny P, Sera R, Leffler R, Barkley M (1999) Genetic variation in susceptibility to endocrine disruption by estrogen in mice. Science 285:1259–1261
36. Stuart RO, Bush KT, Nigam SK (2001) Changes in global gene expression patterns during development and maturation of the rat kidney. Proc Natl Acad Sci U S A 98:5649–5654
37. Turk R, 't Hoen PAC, Sterrenburg E et al (2004) Gene expression variation between mouse inbred strains. BMC Genomics 5:57
38. Van der Weyden L, Adams DJ, Bradley A (2002) Tools for targeted manipulation of the mouse genome. Physiol Genomics 11:133–164
39. Vandesompele J, De Preter K, Pattyn F et al (2002) Accurate normalization of real-time quantitative RT-PCR data by geometric averaging of multiple internal control genes. Genome Biol 3: Research34
40. Walker JR, Su AI, Self DW et al (2004) Applications of a rat multiple tissue gene expression data set. Genome Res 14:742–749
41. Yamamoto T, Sasaki S, Fushimi K et al (1997) Expression of AQP family in rat kidneys during development and maturation. Am J Physiol 272:F198–F204
42. Yasui M, Marples D, Belusa R et al (1996) Development of urinary concentrating capacity: role of aquaporin-2. Am J Physiol 271:F461–F468
43. Yaylaoglu MB, Titmus A, Visel A et al (2005) Comprehensive expression atlas of fibroblast growth factors and their receptors generated by a novel robotic in situ hybridization platform. Dev Dyn 234:371–386
44. Yun J, Schöneberg T, Liu J et al (2000) Generation and phenotype of mice harboring a nonsense mutation in the V2 vasopressin receptor gene. J Clin Invest 106:1361–1371
45. Zhai XY, Fenton RA, Andreasen A, Thomsen JS, Christensen EI (2007) Aquaporin-1 is not expressed in descending thin limbs of short-loop nephrons. J Am Soc Nephrol 18:2937–2944
46. Zhang QJ, Chadderton A, Clark RL, Augustine-Rauch KA (2003) Selection of normalizer genes in conducting relative gene expression analysis of embryos. Birth Defects Res A Clin Mol Teratol 67:533–544